Journal of The Electrochemical Society, **152** (7) G560-G566 (2005)
0013-4651/2005/152(7)/G560/7/$7.00 © The Electrochemical Society, Inc.

Influence of Humidity on Electrical Characteristics of Self-Assembled Porous Silica Low-*k* Films

T. Kikkawa,[a,*,z] S. Kuroki,[a] S. Sakamoto,[a] K. Kohmura,[b] H. Tanaka,[b] and N. Hata[c]

[a]*Research Center for Nanodevices and Systems, Hiroshima University, 1-4-2 Kagamiyama, Higashi-Hiroshima, Hiroshima, 739-8527, Japan*
[b]*MIRAI, Association of Super-Advanced Electronics Technology, 16-1 Onogawa, Tsukuba, Ibaraki 305-8569, Japan*
[c]*MIRAI, Advanced Semiconductor Research Center, National Institute of Advanced Industrial Science and Technology, 16-1 Onogawa, Tsukuba, Ibaraki 305-8569, Japan*

The influence of humidity on the dielectric constant and leakage current of self-assembled porous silica films which have two-dimensional hexagonal periodic porous structures was investigated quantitatively by proposing a new water adsorption model. The amount of H_2O adsorption was calculated by the modified Rayleigh model, where H_2O molecules are assumed to be adsorbed on the inner surface of cylindrical porous silica structures and form a dispersal concentric double-layer dielectric cylinder system. The amount of H_2O calculated by the proposed model was consistent with the measured dielectric constant and thermogravimetry data. It suggests that inner-surface coverage of the cylindrical porous silica wall with a hydrophobic group is the most effective way to suppress water adsorption. Hexamethyldisilazane as a surface coverage molecule was introduced to the periodic cylindrical porous silica film and the leakage current was suppressed by a factor of 1/100 even below 0.5% relative humidity, resulting in the improvement of time-dependent dielectric breakdown lifetime by a factor of 30.
 [DOI: 10.1149/1.1931428]

Manuscript submitted September 2, 2004; revised manuscript received January 19, 2005. Available electronically June 10, 2005.

Scaling of interconnects in ultralarge-scale integrated circuits (ULSI) has caused the increase of signal delay time due to the increase of interconnect resistance (R) and its parasitic capacitance (C),[1] while the transistor scaling is still effective to reduce the gate delay time.[2] For a 1-mm-long interconnect line fabricated on a Si chip, the RC delay time becomes a few hundred picoseconds, which is approximately 10 times larger than that of a metal oxide semiconductor field effect transistor (MOSFET). The RC delay time increases with decreasing the thickness and width of the metal interconnect as well as the spacing. In order to overcome this problem, copper and low-k interlayer dielectrics have been introduced. The interlayer dielectric films with the dielectric constants $k \leqslant 2.0$ are required for future ULSI beyond 45 nm technology node. From the material point of view, various porous films have been developed to lower the dielectric constants.[3] However, the porous low-k films absorb moisture, resulting in the degradation of the film properties. To avoid this problem, a hexamethyldisilazane (HMDS) treatment has been commonly used to make the film hydrophobic.

In this study, the influence of water adsorption on the dielectric constant and leakage current in the porous silica films[4] are investigated quantitatively, and the effect of HMDS treatment is discussed.

Experimental

p-Type Si substrates were cleaned in an RCA solution ($NH_4OH:H_2O_2:H_2O$ = 36:720:1680) and dipped into a 0.5% HF solution. They were oxidized in O_2 ambient at 900°C to form 5 nm thick SiO_2.

A precursor solution for porous silica films was prepared by adding a surfactant, which was a PEO (polyethylene oxide)-PPO (polypropylene oxide)-PEO triblock copolymer and an acidic silica sol derived from tetraethyl orthosilicate (TEOS) in ethanol diluted with water. The precursor solution was spin-coated on a Si substrate to form a homogeneous thin layer. After prebaking at 100°C for 1 h, the sample was calcined in dry air at 400°C for 3 h to burn out the surfactant and to stabilize the chemical structure of the film. Resulting porous silica film thickness was 200 nm. The porous silica film was treated in HMDS ambient at 23°C for 24 h. Si-OH bonds turned into Si-O-Si$(CH_3)_3$ bonds.[5] Aluminum electrodes were formed on the porous silica film as well as the bottom of the Si substrate by direct current magnetron sputtering for electrical characterization. Molecular bonds in the film were measured by Fourier transform infrared spectroscopy (FTIR). The film thickness and refractive index were measured by spectroscopic ellipsometry. The film structure was analyzed by transmission electron microscopy (TEM) and X-ray scattering and diffraction measurements. X-ray source was 0.154 nm Cu Kα. The MOS capacitors were baked at 200°C for 4 h in N_2 ambient before measurement to get rid of water in the films. Then, C-V and I-V measurements were carried out in various humid conditions. Time-dependent dielectric breakdown (TDDB) tests were carried out at 2.9 MV/cm in N_2 at 200°C for the reliability investigation.

The amount of water adsorption in the porous silica film was calculated by various models and compared with the results of thermogravimetry and differential thermal analysis (TG-DTA). C-V and I-V measurements for Al/porous-silica/SiO_2/Si MOS capacitors were carried out in a nitrogen purged shield box as shown in Fig. 1.[6]

Results

Figure 2 shows cross section and plan-view TEM micrographs of the porous silica film. Two-dimensional hexagonal periodic porous structure was clearly observed in Fig. 2a. The enlarged micrograph shows that the shape of a pore is elliptic. This is attributed to the vertical volume shrinkage of the porous film after calcination process at 400°C. Average periodic spacing of the porous silica film normal to the Si substrate was 7.3 nm.

Long cylindrical rods of silica were observed in Fig. 2b and average longitudinal dimension of pores are in the range of 50-100 nm. Therefore, the porous silica film has a periodic hexagonal arrangement of cylindrical pores whose average diameter is approximately 7.3 nm and longitudinal dimension is approximately 50-100 nm. Both hexagonal and lamellar cross sections were also observed, and the lengths of lamellar cross sections were in the range of approximately 50-100 nm as shown in Fig. 2a. The ratio of pore diameter to length is approximately 1/10, so that the pore structure can be modeled as a cylinder and the cylindrical model is more appropriate than random distribution of spheres.

X-ray scattering and diffraction spectra of a self-assembled porous silica film with or without HMDS treatment is shown in Fig. 3. Critical angles of surface scattering and the interface scattering at low-k/Si are $\theta c_{surface} = 0.2°$ and $\theta c_{Si} = 0.4°$, respectively. Diffrac-

* Electrochemical Society Active Member.
z E-mail: kikkawa@sxsys.hiroshima-u.ac.jp

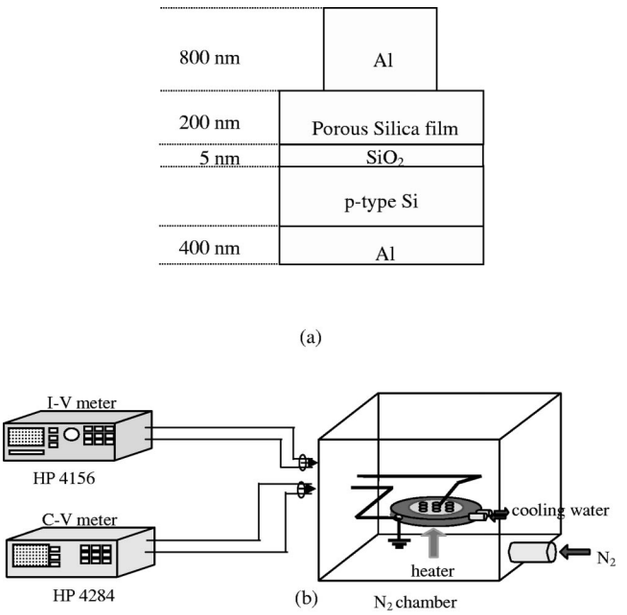

Figure 1. Schematic diagram of a sample and measurement setup. (a) A sample structure. (b) Measurement setup for MOS capacitor.

tion angles corresponding to the periodic hexagonal structure are $2\theta_{100} = 1.1°$ and $2\theta_{200} = 2.2°$, resulting in d spacing of 8 nm, which was close to that of TEM observation.

The pore structure and periodicity remains almost unchanged after the HMDS treatment. Figure 4 shows FTIR spectra before and after HMDS treatment. A C-H peak appeared after the HMDS treatment. Furthermore, the O-H peak decreased after the HMDS treatment. Consequently, it was confirmed that Si-OH bonds were turned into Si-O-Si$(CH_3)_3$ bonds by the HMDS treatment. Figure 5 shows the dielectric constant of the periodic porous silica film as a function of relative humidity (RH). The effect of the HMDS treatment on the dielectric constant versus humidity was clearly observed. The dielectric constant was calculated by the accumulation capacitance of MOS *C-V* curve. The measured lowest dielectric constant of the porous silica film was 2.6 at 0.5% RH, which was consistent with the calculated data from the Lorentz-Lorenz equation. The measured refractive index of the porous silica film was 1.23, so that the porosity of the film was approximately 50% according to the Lorentz-Lorenz equation as expressed in Eq. 1

$$x = 1 - \left(\frac{n_{film}^2 - 1}{n_{film}^2 + 2}\right) \Big/ \left(\frac{n_{SiO2}^2 - 1}{n_{SiO2}^2 + 2}\right) \qquad [1]$$

where x is the porosity of the porous film; n_{film} and n_{SiO2} are average refractive index of the porous film and the refractive index of SiO_2, respectively. The calculated dielectric constant of the periodic cylindrical pore structure was approximately 2.6 assuming a series model of capacitors.

The dielectric constant increased with increasing humidity. The increase of the dielectric constant of porous silica film could be suppressed by the HMDS treatment. This is attributed to the fact that the inner surfaces of the porous silica shown in Fig. 2 are covered with HMDS so that water adsorption in the porous silica was suppressed. Figure 6 shows the effect of HMDS on the leakage current at 1.33 MV/cm as a function of humidity. It was found that HMDS could reduce the leakage current of the porous film in humid environment by approximately 1/100. Furthermore, HMDS can suppress the leakage current of the porous silica films even at very low RH less than 0.5%, suggesting the passivation effect of HMDS on the porous silica surface. The leakage current of the porous silica without HMDS treatment increased exponentially, while that with HMDS treatment increased linearly with humidity.

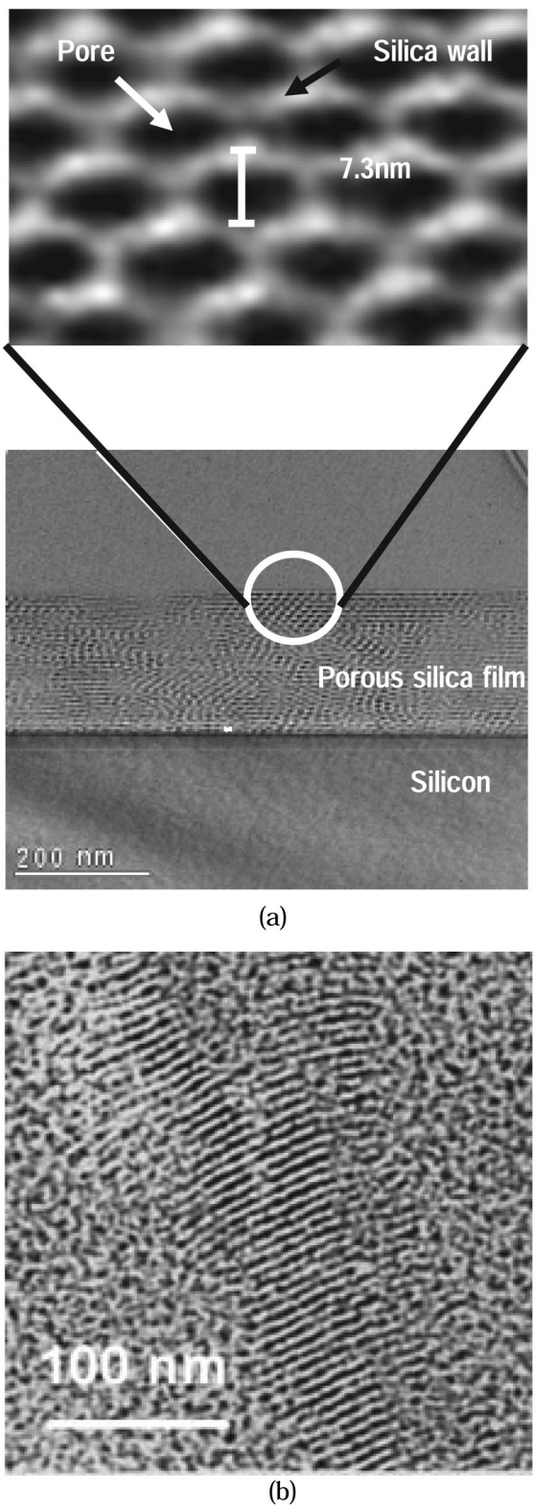

Figure 2. TEM micrographs of a self-assembled porous silica film. (a) Cross-sectional view. Enlarged picture is inserted, showing hexagonal arrangement of elliptical pore structure with d spacing of 7.3 nm. (b) Plan view, showing periodic cylindrical porous silica rods.

It is known that the leakage current in SiO_2 film is generated

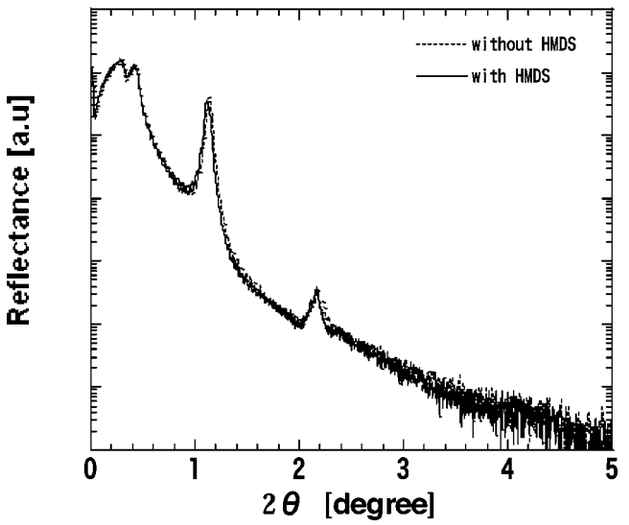

Figure 3. X-ray scattering and diffraction spectra of a self-assembled porous silica film with or without HMDS treatment. Critical angles of surface scattering and interface scattering at low-k/Si are $\theta c_{surface} = 0.2°$ and $\theta c_{Si} = 0.4°$, respectively. Diffraction angles corresponding to the periodic hexagonal structure are $2\theta_{100} = 1.1°$ and $2\theta_{200} = 2.2°$, resulting in d spacing of 8 nm.

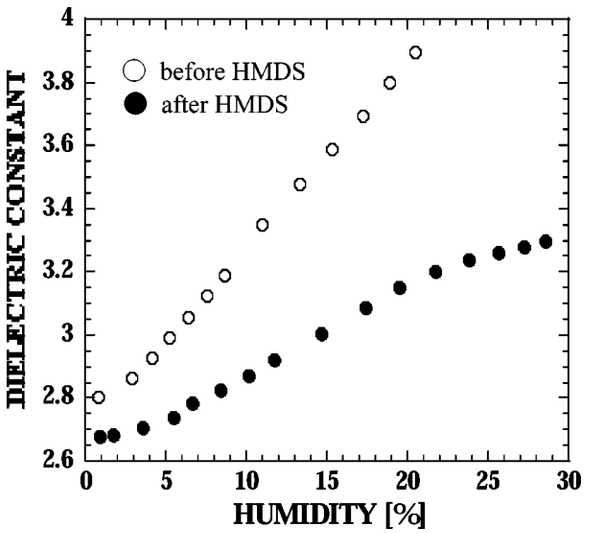

Figure 5. Effect of HMDS treatment on the dielectric constant as a function of humidity. Open circle stands for before HMDS and closed circle stands for after HMDS treatment.

mainly by the Poole-Frenkel mechanism. However, the leakage current of the porous silica film in the humid environment is much larger than that of the bulk SiO_2 film and affected by the humidity. Therefore, we assume the cause of leakage current is dominated by surface current rather than the bulk current. In order to analyze the leakage current mechanisms, Poole-Frenkel and Schottky models are applied.

Figures 7 and 8 show the Schottky and Poole-Frenkel plots, respectively. The effective dielectric constants can be calculated from the linear relationships of $\ln(J/T^2)$-$E^{0.5}$ and $\ln(J/E)$-$E^{0.5}$ to determine the Schottky or Poole-Frenkel mechanism. The Schottky mechanism was more dominant for the porous silica film with the HMDS treatment so that the effective dielectric constants in Fig. 7 ranged from 3 to 4, which were consistent with the results in Fig. 5. Consequently, the leakage current of the porous silica film with the HMDS treatment was not limited by the traps due to the defects in the silica film but by the barrier height at the interface between the metal electrode and the porous silica, indicating the passivation effect of HMDS on the porous silica film. The leakage currents of the porous silica films without the HMDS treatments in the humid conditions could not be explained by either Schottky or Poole-Frenkel mechanism. It could be interpreted by assuming the adsorption of water at the inner surfaces of the porous silica.[7] When the porous silica film absorbs moisture, the defects of the inner surfaces of the porous silica film are terminated by O-H group or H_2O cluster so that more current flows along the inner surfaces of the porous silica as the humidity becomes higher because of the potential difference. Because the thickness of the hexagonal porous silica wall is approximately 2-4 nm, as shown in Fig. 2, the leakage current through the porous silica wall due to H_2O adsorption could be attributed to the direct tunneling current across the thinner silica walls, which become the barriers between the water clusters adsorbed on silica pore surfaces. Therefore, the more the humidity increases, the less the Schottky mechanism becomes dominant, as shown in Fig. 7.

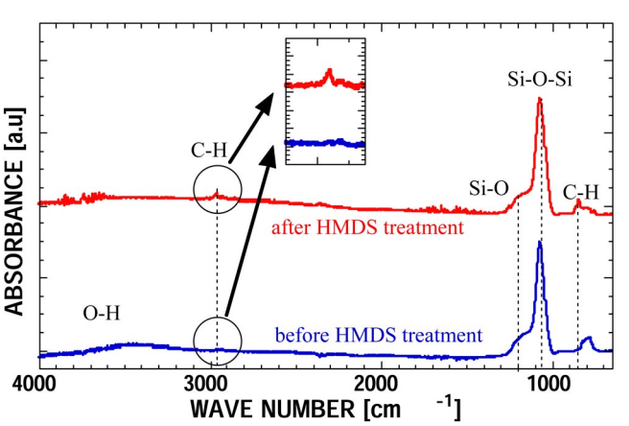

Figure 4. FTIR spectra of porous silica films before and after HMDS. C-H peak due to HMDS is observed and O-H broad peak is diminished after HMDS treatment.

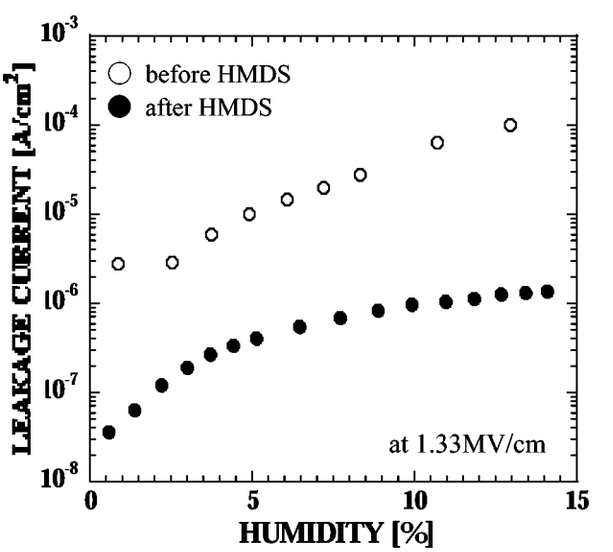

Figure 6. Effect of HMDS treatment on the leakage current at 1.33 MV/cm as a function of humidity. Open circle stands for before HMDS and closed circle stands for after HMDS treatment.

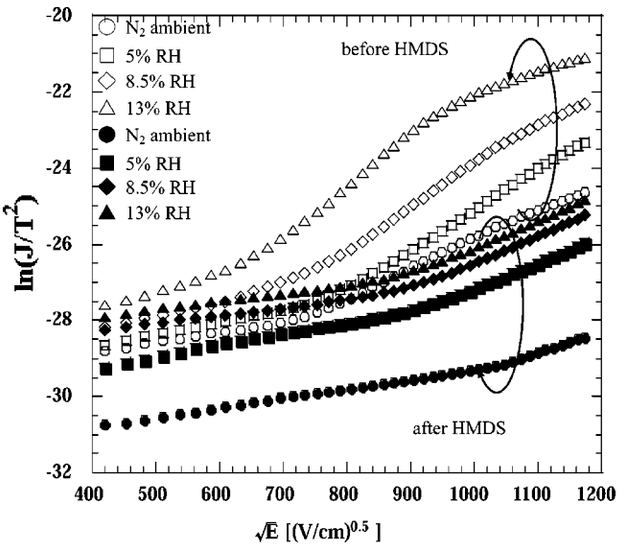

Figure 7. Schottky plot of leakage currents for porous silica films before and after HMDS treatment for relative humidity of 5, 8.5, and 13%. Nitrogen ambient data are shown as a reference. Open patterns stand for before HMDS and closed patterns stand for after HMDS treatment.

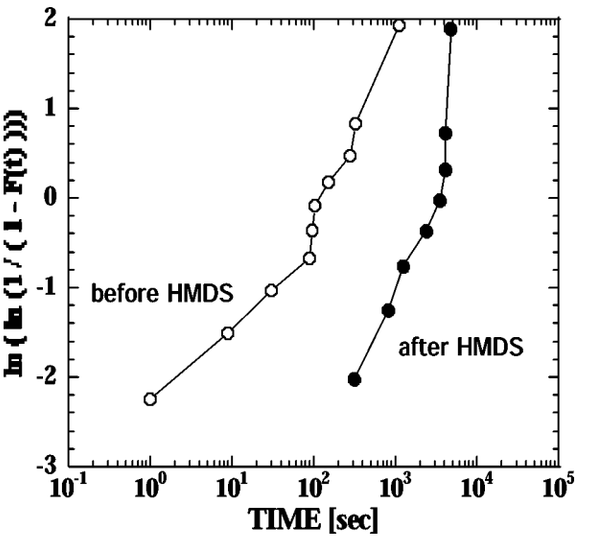

Figure 9. Weibull plot of TDDB lifetime of porous silica films at 2.9 MV/cm in N_2 at 200°C. Effect of HMDS treatment on the TDDB lifetime is shown; open patterns stand for before HMDS and closed patterns stand for after HMDS treatment.

Figure 9 shows the Weibull distribution of the TDDB lifetime at 2.9 MV/cm in N_2 at 200°C for the porous silica films before and after HMDS treatment. It was found that the HMDS treatment could improve the reliability of porous silica film, and the average lifetime of the HMDS-treated porous silica film was improved by a factor of 30. This could be attributed to the passivation effect of HMDS, resulting in homogeneous current flow in the porous silica bulk. Without HMDS passivation, localized currents flow across the thinner parts of the porous silica wall, resulting in inhomogeneous current flow.

Discussion

The amount of adsorbed H_2O was calculated from measured dielectric constants by five different possible models such as series model, parallel model, effective medium approximation (EMA) model,[8] Rayleigh model, and modified Rayleigh model, as shown in Fig. 10a, b, c, d, and e, respectively.

Series model and parallel model assume that silica, pore (air), and water are distributed in series and in parallel as shown in Fig. 10a and b, respectively. The total dielectric constants of the series and parallel models are expressed by Eq. 2 and 3, respectively

$$\frac{1}{k_{film}} = \frac{(1-x)}{k_{silica}} + \frac{y}{k_{water}} + \frac{(x-y)}{k_{air}} \quad \text{Series model} \qquad [2]$$

$$k_{film} = (1-x)k_{silica} + yk_{water} + (x-y)k_{air} \quad \text{Parallel model} \qquad [3]$$

where k_{film}, k_{silica}, k_{air}, and k_{water} are effective dielectric constant of the film, dielectric constant of silica, dielectric constant of air, and dielectric constant of H_2O, respectively, x is the porosity, and y is

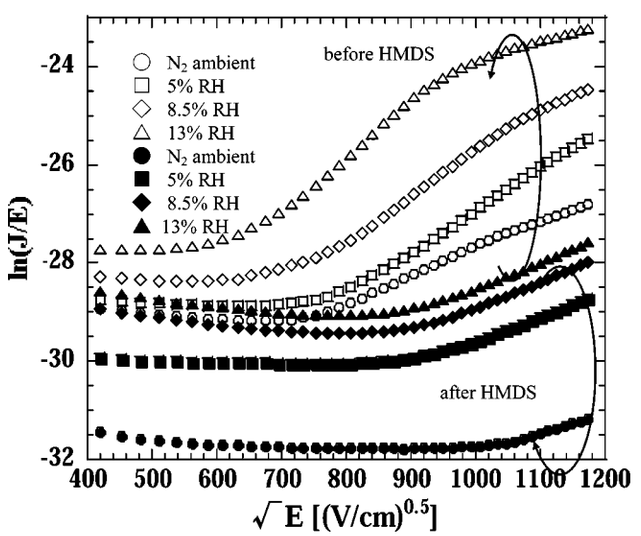

Figure 8. Poole-Frenkel plot of leakage currents for porous silica films before and after HMDS treatment for relative humidity of 5, 8.5, and 15%. Nitrogen ambient data are shown as a reference. Open patterns stand for before HMDS and closed patterns stand for after HMDS treatment.

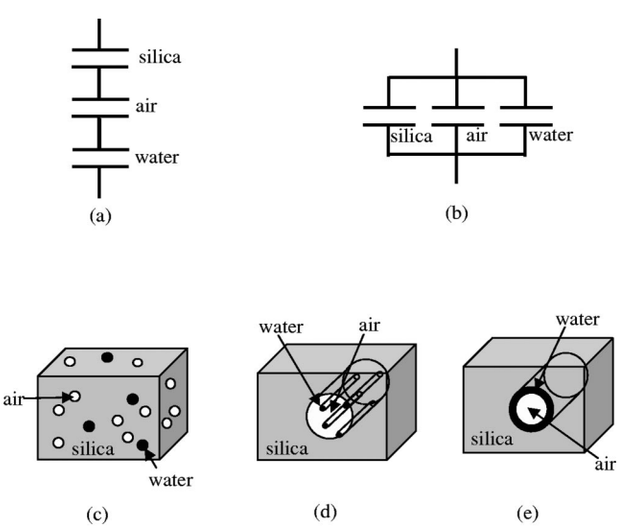

Figure 10. Schematic diagrams of water-adsorbed porous silica models. (a) Series model. (b) Parallel model. (c) EMA model. (d) Rayleigh model. (e) Modified Rayleigh model.

the fraction of adsorbed water. When silica, pore, and H_2O are distributed at random as shown in Fig. 10c, the Clausiuss-Mossotti equation[9] assuming the EMA model should be described as follows

$$\frac{k_{film}-1}{k_{film}+2} = (1-x)\frac{k_{silica}-1}{k_{silica}+2} + (x-y)\frac{k_{air}-1}{k_{air}+2} + y\frac{k_{water}-1}{k_{water}+2} \quad [4]$$

The periodic porous silica has a cylindrical pore structure because hexagonal pores with a diameter of approximately 7.3 nm were observed by cross section TEM in Fig. 2a, and 50-100 nm long silica rods were observed by plan-view TEM in Fig. 2b. Both hexagonal and lamellar cross sections were also observed and the length of lamellar cross sections was in the range of approximately 50-100 nm as shown in Fig. 2a. The ratio of pore diameter to length is approximately 1/10, so the cylindrical model is more appropriate than random distribution of spherical pores.

When cylindrical pores (air) are distributed at random in silica, and water molecules are distributed at random in the cylindrical pore as shown in Fig. 10d, the Rayleigh model can be applied.[10] In this model the shape of water molecules was assumed to be cylinders for two-dimensional approximation of random distribution of water molecules in the pores. The dielectric constant of the film matrix is calculated by the silica and the pore as described in Eq. 5, and the dielectric constant of pore is calculated by the water and the air as expressed in Eq. 6

$$k_{film} = k_{silica}\frac{k_{pore}+k_{silica}+x(k_{pore}-k_{silica})}{k_{pore}+k_{silica}-x(k_{pore}-k_{silica})} \quad [5]$$

$$k_{pore} = k_{air}\frac{k_{water}+k_{air}+\frac{y}{x}(k_{water}-k_{air})}{k_{water}+k_{air}-\frac{y}{x}(k_{water}-k_{air})} \quad [6]$$

where k_{pore} is the dielectric constant of the pore (including air and water).

The Rayleigh model of cylindrical water is not suitable for practical description of water adsorption.[7] When cylindrical pores are distributed at random in the silica, water is adsorbed on the surface of cylindrical pore inner walls[7] as shown in Fig. 10e. We propose a new model called the modified Rayleigh model to express this structure of water adsorption. The equation is expressed as follows

$$k_{pore} = k_{water}\frac{2k_{air}+(k_{water}-k_{air})y/x}{2k_{water}+(k_{air}-k_{water})y/x} \quad [7]$$

The details of calculation are shown in Appendixes A and B. Porosity can be calculated from the effective dielectric constant before moisture uptake, assuming that k_{silica} is 4.0, resulting in $x = 0.271$ for the EMA model and $x = 0.315$ for the Rayleigh model.

Figures 11a and b show calculated volume percentage of water adsorption in the porous film as a function of humidity before and after HMDS treatment, respectively. Water-adsorbed porous silica films are modeled as modified Rayleigh, Rayleigh, EMA, series capacitors, and parallel capacitors. Volume percentages of water adsorption for each model are calculated by Eq. 2-7. It is found that the HMDS treatment could reduce water adsorption, but the amount of water adsorbed in the porous silica film was strongly dependent on the models even for the same measured dielectric constant. The modified Rayleigh model and parallel model show the least water adsorption for the same dielectric constants. The least amount of adsorbed water affects the dielectric constant of the porous film most apparently if the adsorbed water is modeled by the modified Rayleigh model. The modified Rayleigh model could fit well with measured TG-GTA, which was 3.16 vol % of film at 15% RH. It is consistent with the physical model of which the porous silica film has the two-dimensional hexagonal periodic pore structure as shown in Fig. 2, and H_2O molecules are adsorbed on the inner surface of the hexagonally arranged cylindrical wall,[7] resulting in OH termination. This physical model is also consistent with the leakage current mechanism of the porous silica film without HMDS, shown in Fig. 7.

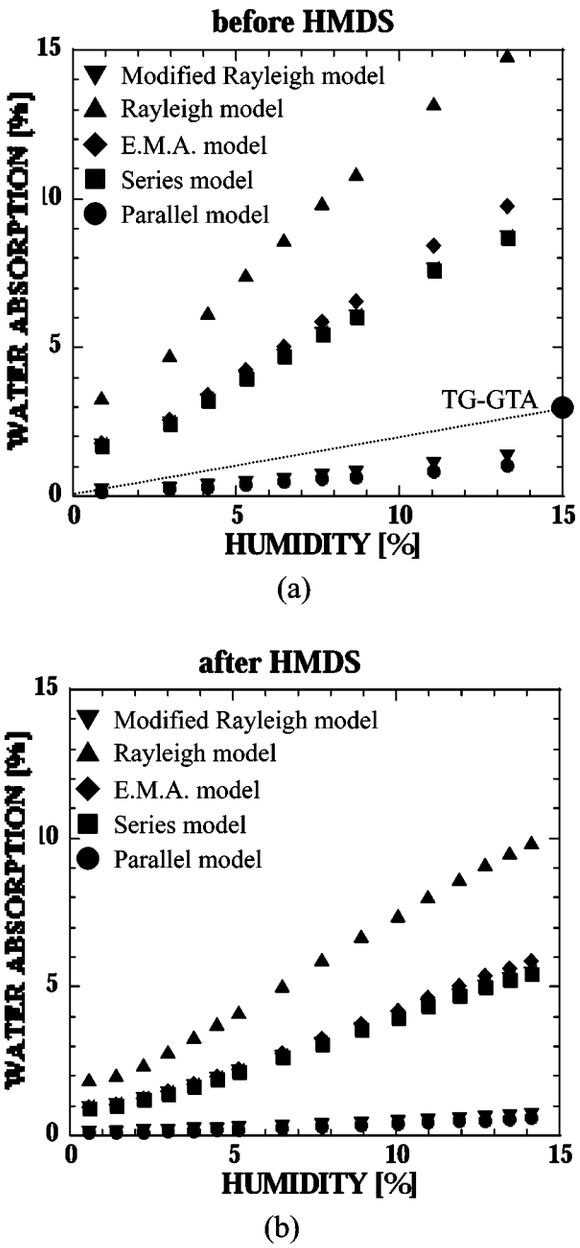

Figure 11. Calculated volume percentage of water adsorption in the porous film as a function of humidity. Water-adsorbed porous silica films are modeled as modified Rayleigh, Rayleigh, EMA, series capacitors, and parallel capacitors. (a) Before HMDS treatment. (b) After HMDS treatment.

Conclusion

The influence of water adsorption on the electrical characteristics of porous silica films was investigated. In order to calculate the amount of H_2O adsorption on the cylindrical porous silica inner surfaces, we proposed an inner surface coverage model named the modified Rayleigh model and compared it with the measured data. The amount of water adsorption calculated from the modified Rayleigh model was consistent with the measurement data, so that this model could be used for water adsorption of self-assembled hexagonal porous silica structures. It is also found that HMDS showed a

passivation effect of the inner surface of cylindrical porous silica so that the leakage current could be reduced by factors of 1/100 even below 0.5% relative humidity, resulting in the improvement of TDDB lifetime by a factor of 30.

Acknowledgments

Part of this work was supported by NEDO and the Ministry of Education, Culture, Sports, Science and Technology under the Grant-in-Aid for Scientific Research. The authors thank Dr. N. Mikami for his useful discussion.

Hiroshima University assisted in meeting the publication costs of this article.

Appendix A
Dispersal Concentric Double-Layer Dielectric Cylinder System

We consider one concentric double-layer dielectric cylinder (external radius: a, internal radius: b) in uniform dielectric medium. Dielectric constants for the region $a < r$, $b < r \leqslant a$, and $r \leqslant b$ are ε_1, ε_2, and ε_3, respectively. First, we derive electrostatic potential of the dielectric under the external electrostatic potential

$$\varphi_0 = -E_0 z = -E_0 r\cos\theta \quad [A\text{-}1]$$

The Laplace equations for each region are written as

$$\Delta\varphi_1 = 0, \quad a < r \quad [A\text{-}2]$$

$$\Delta\varphi_2 = 0, \quad b < r \leqslant a \quad [A\text{-}3]$$

$$\Delta\varphi_3 = 0, \quad r \leqslant b \quad [A\text{-}4]$$

where φ_1 is the electrostatic potential for outside of the dielectric cylinder $a < r$, and φ_2 and φ_3 are the electrostatic potential for inside of the dielectric cylinder $b < r \leqslant a$ and $r \leqslant b$, respectively.

A general solution for Laplace equation in cylindrical coordinates is written as

$$\varphi(r,\theta) = \sum_{n=1}^{\infty} (A_n\cos n\theta + B_n \sin n\theta)\left(C_n r^n + \frac{D_n}{r^n}\right) + (A_0\theta + B_0)(C_0 \log r + D_0) \quad [A\text{-}5]$$

where A_n, B_n, C_n, and D_n ($n = 0,1,2,\ldots$) are constants determined by the boundary conditions

$$\lim_{r\to\infty} \varphi_1 = \varphi_0 \quad [A\text{-}6]$$

$$\varepsilon_1 \left.\frac{\partial \varphi_1}{\partial r}\right|_{r=a} = \varepsilon_2 \left.\frac{\partial \varphi_2}{\partial r}\right|_{r=a} \quad [A\text{-}7]$$

$$\frac{1}{a}\left.\frac{\partial \varphi_1}{\partial \theta}\right|_{r=a} = \frac{1}{a}\left.\frac{\partial \varphi_2}{\partial \theta}\right|_{r=a} \quad [A\text{-}8]$$

$$\varepsilon_2 \left.\frac{\partial \varphi_2}{\partial r}\right|_{r=b} = \varepsilon_3 \left.\frac{\partial \varphi_3}{\partial r}\right|_{r=b} \quad [A\text{-}9]$$

$$\frac{1}{b}\left.\frac{\partial \varphi_2}{\partial \theta}\right|_{r=b} = \frac{1}{b}\left.\frac{\partial \varphi_3}{\partial \theta}\right|_{r=b} \quad [A\text{-}10]$$

Solve these equations, and the electrostatic potentials are given as

$$\varphi_1(r,\theta) = -\left(1 + \gamma\frac{a^2}{r^2}\right)E_0 r\cos\theta, \quad r > a \quad [A\text{-}11]$$

$$\varphi_2(r,\theta) = -\frac{1}{2\varepsilon_2}\left\{(\varepsilon_2 + \varepsilon_3) + (\varepsilon_2 - \varepsilon_3)\frac{b^2}{r^2}\right\}\eta E_0 r\cos\theta, \quad a \geqslant r > b \quad [A\text{-}12]$$

$$\varphi_3(r,\theta) = -\eta E_0 r\cos\theta, \quad b \geqslant r \quad [A\text{-}13]$$

where

$$\gamma \equiv \frac{(\varepsilon_1 - \varepsilon_2)(\varepsilon_2 + \varepsilon_3) + (\varepsilon_1 + \varepsilon_2)(\varepsilon_2 - \varepsilon_3)(1 - y)}{(\varepsilon_1 + \varepsilon_2)(\varepsilon_2 + \varepsilon_3) + (\varepsilon_1 - \varepsilon_2)(\varepsilon_2 - \varepsilon_3)(1 - y)} \quad [A\text{-}14]$$

$$\eta \equiv \frac{4\varepsilon_1\varepsilon_2}{(\varepsilon_1 + \varepsilon_2)(\varepsilon_2 + \varepsilon_3) + (\varepsilon_1 - \varepsilon_2)(\varepsilon_2 - \varepsilon_3)(1 - y)} \quad [A\text{-}15]$$

and y is defined as the volume ratio of cylindrical dielectric shell *vs.* dielectric cylinder

$$y = \frac{\pi(a^2 - b^2)}{\pi a^2} = 1 - \left(\frac{b}{a}\right)^2 \quad [A\text{-}16]$$

The concentric double-layer dielectric cylinder is regarded as a uniform dielectric cylinder that has dielectric constant ε_{eff}, such as the potential ($b \to 0$ limitation of Eq. A-11)

$$\varphi_1(r,\theta) = -\left(1 + \frac{\varepsilon_1 - \varepsilon_{eff}}{\varepsilon_1 + \varepsilon_{eff}}\cdot\frac{a^2}{r^2}\right)E_0 r\cos\theta, \quad r > a \quad [A\text{-}17]$$

This equation is compared to Eq. A-11, and then

$$\varepsilon_{eff} = \frac{1 - \gamma}{1 + \gamma}\varepsilon_1 \quad [A\text{-}18]$$

where

$$\gamma \equiv \frac{(\varepsilon_1 - \varepsilon_2)(\varepsilon_2 + \varepsilon_3) + (\varepsilon_1 + \varepsilon_2)(\varepsilon_2 - \varepsilon_3)(1 - y)}{(\varepsilon_1 + \varepsilon_2)(\varepsilon_2 + \varepsilon_3) + (\varepsilon_1 - \varepsilon_2)(\varepsilon_2 - \varepsilon_3)(1 - y)} \quad [A\text{-}19]$$

This is the effective dielectric constant for concentric double-layer dielectric cylinder. The dielectric constant ε of the medium that has many dispersal concentric double-layer dielectric cylinders is given by Rayleigh's equation of dispersal dielectric cylinders

$$\varepsilon = \varepsilon_1\frac{\varepsilon_1 + \varepsilon_{eff} - x(\varepsilon_1 - \varepsilon_{eff})}{\varepsilon_1 + \varepsilon_{eff} + x(\varepsilon_1 - \varepsilon_{eff})} \quad [A\text{-}20]$$

where ε_1 is the dielectric constant for outside of the dispersal dielectric cylinders, ε_{eff} is the effective dielectric constant for concentric double-layer dielectric cylinder given by Eq. A-18, and x is the total volume ratio of the dispersal dielectric cylinders.

Appendix B
Dispersal Concentric Double-Layer Dielectric Sphere System

We consider one concentric double-layer dielectric sphere (external radius: a, internal radius: b) in uniform dielectric medium. Dielectric constants for the region $a < r$, $b < r \leqslant a$, and $r \leqslant b$ are ε_1, ε_2, and ε_3, respectively. The external electrostatic potential is given as

$$\varphi_0 = -E_0 z = -E_0 r\cos\theta \quad [B\text{-}1]$$

The Laplace equations for each region are written as

$$\Delta\varphi_1 = 0, \quad a < r \quad [B\text{-}2]$$

$$\Delta\varphi_2 = 0, \quad b < r \leqslant a \quad [B\text{-}3]$$

$$\Delta\varphi_3 = 0, \quad r \leqslant b \quad [B\text{-}4]$$

where φ_1 is the electrostatic potential for outside of the dielectric sphere $a < r$, and φ_2 and φ_3 are the electrostatic potential for inside of the dielectric sphere $b < r \leqslant a$ and $r \leqslant b$, respectively.

A general solution for the Laplace equation in spherical coordinates is written as

$$\varphi(r,\theta) = \sum_{l=0}^{\infty}(A_l r^l + B_l r^{-(l+1)})P_l(\cos\theta) \quad [B\text{-}5]$$

where P_l ($l = 0,1,2,\ldots$) is the Legendre polynomial, and A_l and B_l ($l = 0,1,2,\ldots$) are constants determined by the boundary conditions

$$\lim_{r\to\infty} \varphi_1 = \varphi_0 \quad [B\text{-}6]$$

$$\varepsilon_1 \left.\frac{\partial \varphi_1}{\partial r}\right|_{r=a} = \varepsilon_2 \left.\frac{\partial \varphi_2}{\partial r}\right|_{r=a} \quad [B\text{-}7]$$

$$\frac{1}{a}\left.\frac{\partial \varphi_1}{\partial \theta}\right|_{r=a} = \frac{1}{a}\left.\frac{\partial \varphi_2}{\partial \theta}\right|_{r=a} \quad [B\text{-}8]$$

$$\varepsilon_2 \left.\frac{\partial \varphi_2}{\partial r}\right|_{r=b} = \varepsilon_3 \left.\frac{\partial \varphi_3}{\partial r}\right|_{r=b} \quad [B\text{-}9]$$

$$\frac{1}{b}\left.\frac{\partial \varphi_2}{\partial \theta}\right|_{r=b} = \frac{1}{b}\left.\frac{\partial \varphi_3}{\partial \theta}\right|_{r=b} \quad [B\text{-}10]$$

Solve these equations and the electrostatic potentials are given as

$$\varphi_1(r,\theta) = -\left(1 + \gamma\frac{a^3}{r^3}\right)E_0 r\cos\theta, \quad r > a \quad [B\text{-}11]$$

$$\varphi_2(r,\theta) = -\frac{1}{3\varepsilon_2}\left\{(2\varepsilon_2 + \varepsilon_3) + (\varepsilon_2 - \varepsilon_3)\frac{b^3}{r^3}\right\}\eta E_0 r\cos\theta, \quad a \geqslant r > b \quad [B\text{-}12]$$

$$\varphi_3(r,\theta) = -\eta E_0 r\cos\theta, \quad b \geqslant r \quad [B\text{-}13]$$

where

$$\gamma \equiv \frac{(\varepsilon_1 - \varepsilon_2)(2\varepsilon_2 + \varepsilon_3) + (\varepsilon_1 + 2\varepsilon_2)(\varepsilon_2 - \varepsilon_3)(1 - y)}{(2\varepsilon_1 + \varepsilon_2)(2\varepsilon_2 + \varepsilon_3) + 2(\varepsilon_1 - \varepsilon_2)(\varepsilon_2 - \varepsilon_3)(1 - y)} \quad [B\text{-}14]$$

$$\eta \equiv \frac{9\varepsilon_1\varepsilon_2}{(2\varepsilon_1 + \varepsilon_2)(2\varepsilon_2 + \varepsilon_3) + 2(\varepsilon_1 - \varepsilon_2)(\varepsilon_2 - \varepsilon_3)(1 - y)} \quad [B\text{-}15]$$

and y is defined as the volume ratio of spherical dielectric shell versus dielectric sphere

$$y = \frac{\frac{4}{3}\pi(a^3 - b^3)}{\frac{4}{3}\pi a^3} = 1 - \left(\frac{b}{a}\right)^3 \quad [B\text{-}16]$$

Same as the dielectric cylinder, the concentric double-layer dielectric sphere is regarded as a uniform dielectric sphere that has dielectric constant ε_{eff}, such as the potential ($b \rightarrow 0$ limitation of Eq. B-11)

$$\varphi_1(r,\theta) = -\left(1 + \frac{\varepsilon_1 - \varepsilon_{eff}}{2\varepsilon_1 + \varepsilon_{eff}}\frac{a^3}{r^3}\right)E_0 r\cos\theta, \quad r > a \quad [B\text{-}17]$$

This equation is compared to Eq. B-11, and then

$$\varepsilon_{eff} = \frac{1 - 2\gamma}{1 + \gamma}\varepsilon_1 \quad [B\text{-}18]$$

where

$$\gamma \equiv \frac{(\varepsilon_1 - \varepsilon_2)(2\varepsilon_2 + \varepsilon_3) + (\varepsilon_1 + 2\varepsilon_2)(\varepsilon_2 - \varepsilon_3)(1 - y)}{(2\varepsilon_1 + \varepsilon_2)(2\varepsilon_2 + \varepsilon_3) + 2(\varepsilon_1 - \varepsilon_2)(\varepsilon_2 - \varepsilon_3)(1 - y)} \quad [B\text{-}19]$$

This is the effective dielectric constant for the concentric double-layer dielectric sphere.

The dielectric constant ε of the medium that has many dispersal concentric double-layer dielectric spheres is given by Rayleigh's equation of dispersal dielectric spheres

$$\varepsilon = \varepsilon_1\frac{2\varepsilon_1 + \varepsilon_{eff} - 2x(\varepsilon_1 - \varepsilon_{eff})}{2\varepsilon_1 + \varepsilon_{eff} + x(\varepsilon_1 - \varepsilon_{eff})} \quad [B\text{-}20]$$

where ε_1 is the dielectric constant for outside of the dispersal dielectric spheres, ε_{eff} is the effective dielectric constant for concentric double-layer dielectric sphere given by Eq. B-18, and x is the volume ratio of the dispersal dielectric spheres.

References

1. H. B. Bakoglu and J. D. Meindl, *IEEE Trans. Electron Devices*, **32**, 903 (1985).
2. R. H. Dennard, F. H. Gaensslen, H-N. Yu, V. L. Rideout, E. Bassous, and A. R. LeBlanc, *IEEE J. Solid-State Circuits*, **9**, 256 (1974).
3. K. Yamada, Y. Oku, N. Hata, S. Takada, and T. Kikkawa, *Jpn. J. Appl. Phys., Part 1*, **42**, 1840 (2003).
4. S. Sakmaoto, S. Kuroki, and T. Kikkawa, Extended Abstracts of Solid-State Devices and Materials, p. 478, Japan Society of Applied Physics, Tokyo (2003).
5. S. E. Schulz, H. Koerner, C. Murray, I. Streiter, and T. Gessner, *Microelectron. Eng.*, **55**, 45 (2001).
6. A. L. S. Loke, J. T. Wetzel, P. H. Townsend, T. Tanabe, R. N. Virtis, M. P. Zussman, D. Kumar, C. Ryu, and S. S. Wong, *IEEE Trans. Electron Devices*, **46**, 2178 (1999).
7. E. W. Hansen, M. Stocker, and R. Schmidt, *J. Phys. Chem.*, **100**, 2195 (1996).
8. D. E. Aspnes, *Thin Solid Films*, **89**, 249 (1982)
9. C. Kittel, *Introduction to Solid State Physics*, John Wiley & Sons, New York (1986).
10. J. W. Rayleigh, *Philos. Mag.*, **34**, 481 (1892).